MID-AMERICA TRANSPORTATION CENTER

Report # MATC-UI: 142-1

Final Report
WBS:25-1121-0005-142-1

Infrastructure Inspection During and After Unexpected Events - Phase I

Salam Rahmatalla, Ph.D.
Professor
Department of Civil and Environmental Engineering
University of Iowa

Ali Karimpour, MSc
Research Assistant
Department of Civil and Environmental Engineering
University of Iowa

2018

A Cooperative Research Project sponsored by
U.S. Department of Transportation- Office of the Assistant Secretary for Research and Technology

Infrastructure Inspection During and After Unexpected Events – Phase I

Salam Rahmatalla, Ph.D.
Professor
Civil and Environmental Engineering
University of Iowa

Ali Karimpour, MSc
Research Assistant
Civil and Environmental Engineering
University of Iowa

A Report on Research Sponsored by

Mid-America Transportation Center

University of Nebraska-Lincoln

December 2018

TECHNICAL REPORT DOCUMENTATION PAGE

1. Report No. 25-1121-0005-142-1	2. Government Accession No.	3. Recipient's Catalog No.
4. Title and Subtitle Infrastructure Inspection During and After Unexpected Events - Phase I		5. Report Date December 2018
		6. Performing Organization Code
7. Author(s) Salam Rahmatalla https://orcid.org/0000-0003-3889-4364 and Ali Karimpour		8. Performing Organization Report No. 25-1121-0005-142-1
9. Performing Organization Name and Address Mid-America Transportation Center 2200 Vine St. PO Box 830851 Lincoln, NE 68583-0851		10. Work Unit No. (TRAIS)
		11. Contract or Grant No. 69A3551747107
12. Sponsoring Agency Name and Address Office of the Assistant Secretary for Research and Technology 1200 New Jersey Avenue, SE Washington, DC 20590		13. Type of Report and Period Covered Final Report, August 2017 – December 2018
		14. Sponsoring Agency Code MATC TRB RiP No. 91994-12
15. Supplementary Notes		

16. Abstract

This report presents the development of a vibration-based damage-detection methodology for the structural health monitoring and damage detection of vital line structures and highway bridges under extreme conditions, including seismic and water interactions. The damage-detection method uses the transmissibility function—the ratio between the output signals at two locations on the structure—of the acceleration, angular velocity, and strain signals to generate a damage index. The validity of the proposed damage index was tested on a small-scale model of a highway bridge under impact loading, with ground vibration, and inside a water flume. The initial experimental results showed a very promising performance of the proposed damage index in detecting changes in the integrity of the structure under different loading/damage conditions. The results also showed the benefits of deploying heterogeneous kinds of sensors rather than just using one type of sensor.

17. Key Words Structural Health Monitoring (SHM), Damage Detection (DD), Transmissibility Based Damage Detection (TBDD), Highway Bridges.	18. Distribution Statement

19. Security Classif. (of this report) Unclassified	20. Security Classif. (of this page) Unclassified	21. No. of Pages 30	22. Price

Table of Contents

List of Figures

Acknowledgments

The authors would like to thank Charles Harris for his assistance with the data collection process. Also, appreciation is given to Brandon Barquist for fabricating the steel connectors and mounting elements at flume.

Disclaimer

The contents of this report reflect the views of the authors, who are responsible for the facts and the accuracy of the information presented herein. This document is disseminated in the interest of information exchange. The report is funded, partially or entirely, by a grant from the U.S. Department of Transportation's University Transportation Centers Program. However, the U.S. Government assumes no liability for the contents or use thereof.

Abstract

This report presents the development of a vibration-based damage-detection methodology for the structural health monitoring and damage detection of vital line structures and highway bridges under extreme conditions, including seismic and water interactions. The damage-detection method uses the transmissibility function—the ratio between the output signals at two locations on the structure—of the acceleration, angular velocity, and strain signals to generate a damage index. The validity of the proposed damage index was tested on a small-scale model of a highway bridge under impact loading, with ground vibration, and inside a water flume. The initial experimental results showed a very promising performance of the proposed damage index in detecting changes in the integrity of the structure under different loading/damage conditions. The results also showed the benefits of deploying heterogeneous kinds of sensors rather than just using one type of sensor.

Chapter 1 Introduction and Background

As the world is seeing more severe and damaging natural events, the need for methods that can evaluate structural integrity during and after these events is becoming more vital (figs. 1.1-1.2). Structural health monitoring (SHM) and damage-detection techniques are considered the most concerning issues for engineers as well as governments for prolonging infrastructure service life and ensuring public safety [1-4]. SHM is the process of implementing a paradigm for continuously monitoring and supervising the structure's integrity with highest reliability. Different types of sensors can be used to monitor the changes in the integrity of the structures; accelerometers and strain gauges are examples.

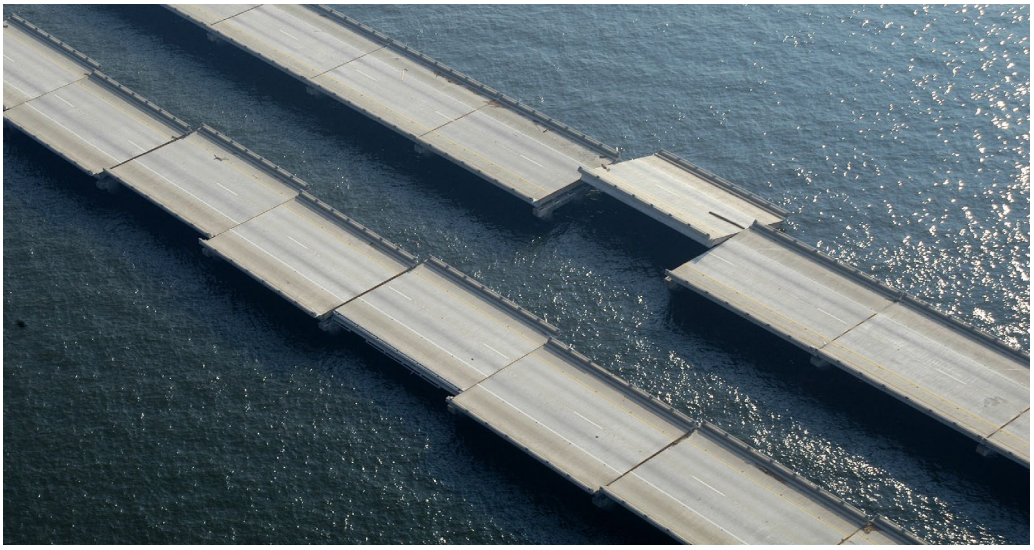

Figure 1.1 Collapse due to unpredicted wave loads on the bridge superstructure during an extreme event.

Figure 1.2 Collapse due to huge loading on the partially drifted deck after extreme event.

Vibration-based damage-detection methodologies (VBDT) have become more popular during the last two decades [5-10]. VBDT has been shown to be very effective in capturing the global and local changes in the structural integrity that can happen because of the changes in the stiffness, mass, and damping properties of the structure. Different types of VBDT algorithms have been introduced in the literature and have shown different performances and limitations. While accelerometers are traditionally used in VBDT methods, different types and combinations of sensors were also used, including strain gauges.

Wang et al. [9] proceeded, performed, and compared damage-detection analysis of a bridge model using two different types of sensors, accelerometers, and strain gauges. In that work, the sensitivity of parameters in two conditions (healthy and damaged) of a bridge model was studied. The coordinate modal assurance criterion (COMAC) values of the strain modes showed differences at the damaged location, while acceleration COMAC were unable to do so. Lee et al. [10] proposed a damage-detection method using the frequency response function (FRFs) measurements from combined acceleration and strain signals. The general formulas for

computing the displacement FRF and strain FRF and their relationships were derived. Then, the method was investigated on a simple supported beam and showed promising results. Although the method could detect several damage scenarios, several restrictions were still presented; the theoretical differential equation of motion corresponding to the beam must be solved separately before applying the damage-detection method. This means that some accurate priori information about the system and its mode shapes was needed to obtain meaningful results.

Recently, the interest in using the transmissibility function, as one type of VBDT method, in detecting damage on structures has greatly increased [11-17]. The transmissibility function can be calculated using the response ratio between two sensors on the structures. The transmissibility function has been shown to be more sensitive to local changes in the dynamic integrity of the structure as compared to the popular frequency response function (FRF). One study [17] suggested using a damage-detection methodology based on strain transmissibility functions to precisely diagnose local damage. Experimental and numerical results were prosperous on a clamped-clamped steel beam. However, the only damage scenario that was considered was to add extra masses on the beam. It was proved that strain mode shapes were more sensitive to mass changes than displacement.

Maia et al. [13] proposed a transmissibility damage indicator developed from two previous criterions, the response vector assurance criterion plus the detection and relative quantification. They examined the proposed method on a clamped beam numerically as well as experimentally. Their indicator was more sensitive to some damage scenarios than the conventional one. Zhou et al. [14] applied the Mahalanobis distance instead of the Euclidean distance to quantify differences between intact and damaged transmissibility terms. The well-known Mahalanobis distance metric has a specific virtue because it takes correlation among

variables into account. Zhou et al. [14] also proposed a new metric named “advanced resulting index based on Mahalanobis concept”. Although the new indicator was experimentally successful in detecting several damage scenarios simulated on a free-free steel beam as a model, the method was unable to correctly sense the intensity of the simulated damages even on a simple physical model. Zhou et al. [15] derived formulations of relationships between the transmissibility coherence and FRF coherence and then employed them to develop accumulated transmissibility coherence as well as a transmissibility modal assurance criterion. They examined the method on a small physical model and claimed that the method was able to detect nonlinearity as well.

Schallhorn et al. [18-19] proposed coherence-based transmissibility damage detection to successfully diagnose simulated damage on highway bridges. In that algorithm, in order to reduce the effect of noisy data and achieve reliable alarms, the damage indicator was calculated alongside a frequency band of interest which encompassed high coherency. Schallhorn et al. also inserted statistical approaches to minimize false alarms due to noise and environmental effects. Their method could detect different types of damage scenarios such as crack growth around retrofit cracks.

In this work, a damage-detection method, based on the transmissibility function, will be introduced. The proposed method uses different types of sensors, including accelerometers, gyroscopes, and strain gauges. The effectiveness of the proposed method will be tested on a model of a highway bridge under three types of loading: impact loading, simulated earthquake loading on a shaker table, and a simulated flooding condition inside a water flume. First, a highway bridge in Iowa was chosen as a prototype bridge, which represents the most common type of mid-size bridge in the U.S. Second, a finite element model (FEM) of the bridge model,

based on the original maps of the bridge, was simulated inside the commercial finite element program ANSYS. Third, a small scaled model of the prototype bridge was built after reviewing the as-built plans of the prototype bridge provided by the Iowa DOT. Finally, several damage scenarios defined and simulated in the computer and in the laboratory were considered.

Chapter 2 Damage-Detection Algorithm

In this section, a vibration-based damage-detection methodology is introduced. The proposed method consolidates information from different types of sensors to generate a damage-detection index called the "effective damage index." The new damage index is expected to add novel aspects to data analysis in pursuit of a more effective localized vibration-based damage-detection algorithm that could be implemented on different structures. The proposed method will be tested under three types of loading: an impact test, on a shaker table, and in a water flume. The proposed method is an output-only approach that does not require information about the input force to the system.

2.1 Equation of Motion and Dynamic Functions

The equation of motion for a general mechanical system can be written in the following form:

$$M\ddot{x}(t) + C\dot{x}(t) + K\,x(t) = F(t) \tag{2.1}$$

where M is the mass matrix of the system; C is the damping matrix; K is the stiffness matrix; $\ddot{x}(t)$, $\dot{x}(t)$, $x(t)$ are the acceleration, velocity, and displacement vectors, respectively; and $F(t)$ is the external force vector.

The FRF is the ratio of a response at a degree of freedom (a certain location on the structure) to the imposed force at either the same or another degree of freedom. For a multi-degree-of-freedom system, instead of having one element, there is a matrix ($H_{ij)}$ representing FRF:

$$H_{ij}(\omega) = \frac{X_i(\omega)}{F_j(\omega)} \tag{2.2}$$

where ω is the frequency of vibration, X_i is the response at location i, and F_j is the applied load at location j.

The transmissibility function (TR) can be expressed as the ratio of the cross-spectrum density $G_{ij}(\omega)$ and power spectrum density $G_{jj}(\omega)$ between two responses on the structure, as follows [6-8]:

$$T_{ij}(\omega) = \frac{G_{ij}(\omega)}{G_{jj}(\omega)} \tag{2.3}$$

Another essential term in signal processing for structural dynamics is the coherence function (CF), which is similar to a statistical function. In fact, each CF indicates correlation as well as linearity of two time-domain signals in the frequency domain and is defined as follows [6-7, 18-19]:

$$\gamma_{ij}(\omega) = \frac{\left|G_{ij}(\omega)\right|^2}{G_{ii}(\omega)G_{jj}(\omega)} \tag{2.4}$$

where $\gamma_{ij}(\omega)$ is the CF. It is obvious that the range of the CF is from zero for completely uncorrelated signals to unity for strongly correlated ones. If the signals are contaminated by noise or any alien vibrating source in their respective bandwidths, the CF tends to abate along those bands.

2.2 Conventional Transmissibility-Based Damage-Detection Index

In order to detect damage effectively, features extraction and statistical classifications are required to convert the sensor's raw data to a specific damage index. In the feature extraction methods, the goal is to compare the mode shapes and natural frequencies of intact and damaged structures. Inversely, in the conventional transmissibility-based damage index, the method does not need any specific information about the system's modal properties. In the conventional

transmissibility method, the first step would be to establish a baseline transmissibility for the healthy structure. However, transmissibility varies widely alongside the frequency band and can be sensitive to the magnitude of energy and noise across the frequencies. Second, a high coherency bandwidth for each transmissibility must be picked up. Finally, by comparing the transmissibility signal between intact (healthy) and damaged structures alongside the high coherence bandwidth, damage could be diagnosed effectively. The damage index (DI) in these methods is usually defined as follows [12,17-21]:

$$DI_{ij(k)} = \left| \sum_{\omega} \frac{\left| \ln \left| T^{H}_{ij(k)}(\omega) \right| - \ln \left| T^{D}_{ij(k)}(\omega) \right| \right|}{\ln \left| T^{H}_{ij(k)}(\omega) \right|} \right| \tag{2.5}$$

where $DI_{ij(k)}$ is the damage indicator value, $T^{D}_{ij(k)}(\omega)$ is the damaged transmissibility function for the comparison to the intact one, $T^{H}_{ij(k)}(\omega)$ is the intact transmissibility between the i-th and j-th DOFs while loading is at the k-th DOF over the high coherency bandwidths, and "ln" is the natural logarithm. Using this formula, at each high coherency frequency band, the normalized difference would be reported as DI.

2.3 Effective Damage Index of Multi-Sensors

If "m" number of sensors is being deployed in a damage-detection process, regardless of the type of each signal, the total transmissibility matrix (TR) can be defined as follows:

$$TR(\omega) = \begin{bmatrix} Tr_{11} & \cdots & Tr_{1m} \\ Tr_{21} & \ddots & \\ \vdots & & \\ Tr_{m1} & \cdots & Tr_{m1} \end{bmatrix}_{m*m} \tag{2.6}$$

From each element of this matrix, a damage index can be produced similar to that in Eq. 2.5. In this study, three types of signals from three different sensors were exploited. Using

accelerometers, gyroscopes, and strain sensors, the following transmissibility terms can be produced respectively:

$$ {}^{\ddot{X}\ddot{X}}T_{ij(k)}(\omega) = \frac{\ddot{X}_{ik}(\omega)}{\ddot{X}_{jk}(\omega)} \tag{2.7} $$

$$ {}^{\dot{\theta}\dot{\theta}}T_{ij(k)}(\omega) = \frac{\dot{\theta}_{ik}(\omega)}{\dot{\theta}_{jk}(\omega)} \tag{2.8} $$

$$ {}^{\varepsilon\varepsilon}T_{ij(k)}(\omega) = \frac{\varepsilon_{ik}(\omega)}{\varepsilon_{jk}(\omega)} \tag{2.9} $$

where $\ddot{X}_{ik}(\omega)$, $\dot{\theta}_{ik}(\omega)$, $\varepsilon_{ik}(\omega)$ are the acceleration, angular velocity, and strain signal responses at the i-th DOF due to the imposed force at the k-th DOF, respectively; and $\ddot{X}_{jk}(\omega)$, $\dot{\theta}_{jk}(\omega)$, $\varepsilon_{jk}(\omega)$ are the acceleration, angular velocity, and strain signal responses at the j-th DOF due to the imposed force at the k-th DOF, respectively. Also, ${}^{\dot{\theta}\dot{\theta}}T_{ij(k)}(\omega)$, ${}^{\ddot{X}\ddot{X}}T_{ij(k)}(\omega)$, and ${}^{\varepsilon\varepsilon}T_{ij(k)}(\omega)$ are the TR functions of the auto angular velocity, auto acceleration, and auto strain between the i-th and j-th DOFs due to the imposed force at the k-th DOF, respectively. For each of these three transmissibility terms, the coherence function can be estimated by Eq. (2.4).

Damage indices $DI_{\dot{\theta}\dot{\theta}}$, $DI_{\ddot{X}\ddot{X}}$, and $DI_{\varepsilon\varepsilon}$ from the latter three TRs can be calculated by Eq. (2.5) alongside each term's high coherency bandwidth. Finally, the effective DI would be the summation of these three DIs as follows:

$$ DI_{effective} = DI_{\dot{\theta}\dot{\theta}} + DI_{\ddot{X}\ddot{X}} + DI_{\varepsilon\varepsilon} \tag{2.10} $$

2.4 Modeling of the Testbed

It is essential to construct a testbed to simulate different damage scenarios as well as to verify the proposed damage-detection method before using it on prototype structures [22]. For this purpose, a small-scale model of the structure prototype was created. A highway bridge in Iowa (FHWA#31690) was chosen as a prototype structure, which represents the most common type of mid-size bridge in the USA. The bridge is a composite steel I-girder and a concrete deck with a single span of 18.6 m (61 ft) carrying Highway 1 over a small natural creek in Johnson County, Iowa (fig. 2.1a). As-built blueprints and updated rehabilitation plans of the prototype were provided by the Iowa DOT (fig. 2.1b). This type of highway bridge could be a fair representative of vital line structures in which each span of the bridge acts almost independently from other spans [23]. The scale factor for the model of the bridge was chosen to be large enough to allow the installation of various sensors, as well as small enough so that it can be fitted and tested inside the water flume. Additionally, the model was geometrically similar to the prototype bridge. The CAD file of the scaled model was created from as-built blueprints of the prototype bridge using a scale factor of 1:25 (fig. 2.1c).

Two kinds of materials were chosen in the bridge model design and fabrication: (1) stainless steel was used for the bridge girder, cross beams, and support connection; and (2) aluminum was used for the bridge deck. Each element of the model was connected by bolts and nuts. Simulating different kinds of damage scenarios was achieved by fastening or loosening a specific part of the model. Girders, cross beams, and innovative support connections were manufactured by 3D printer technology provided by commercial companies in the USA; the deck was precisely cut by Water-Jet Technology (fig 2.1d).

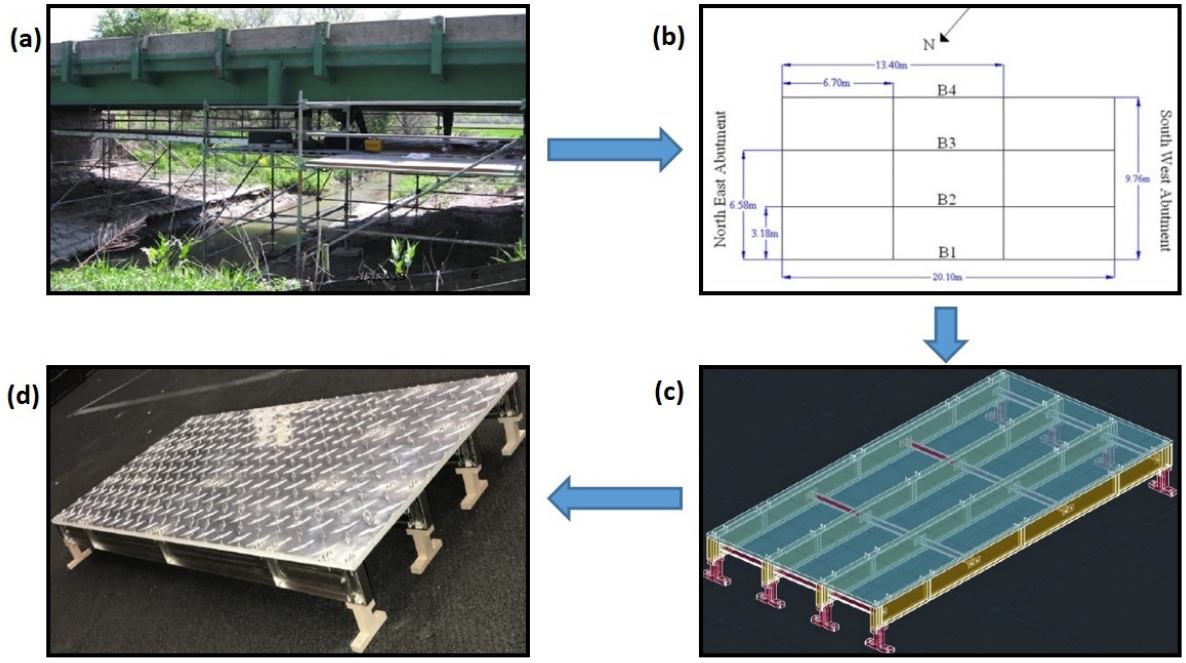

Figure 2.1 Configuration of the modeling process from prototype to small scaled model; (a) view of single-span bridge (FHWA#31690); (b) schematic of the grid system of its composite beam; (c) the CAD model; (d) the physical small scaled model.

Chapter 3 Numerical Modeling and Analysis:

A finite element model of the bridge model was established inside the commercial finite element software ANSYS, as shown in figure 3.1. As can be seen from the figure, the bridge superstructure is sitting on 8 supports that are rigidly attached to the ground. The finite element model was excited by an impulse force to simulate broadband excitation at location “B” at the center of the bridge, as shown in figure 3.1. Two types of responses, acceleration and angular velocity signals, were collected at location “A” at the upper corner of the left side support and at location “B”. Therefore, point “B” can be considered as the location for the input force as well as the first output location. Location “A” is considered to be the second output location. Figure 3.2 shows the first four mode shapes of the bridge.

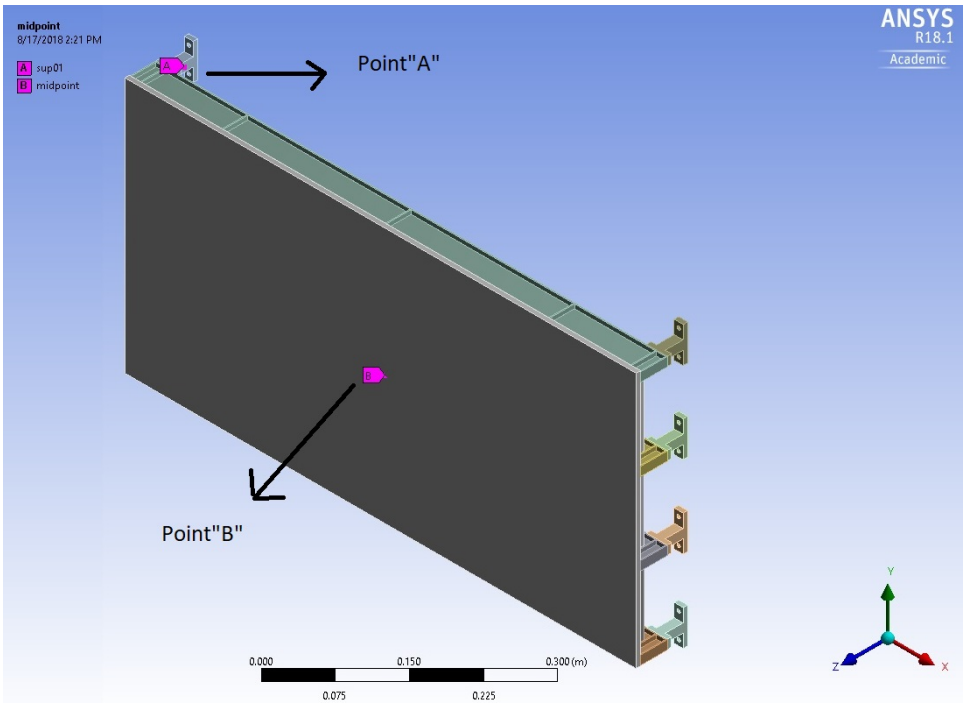

Figure 3.1 Configuration of the FE model; Point “B” is the input as well as 1st output location, Point “A” is the 2nd output location.

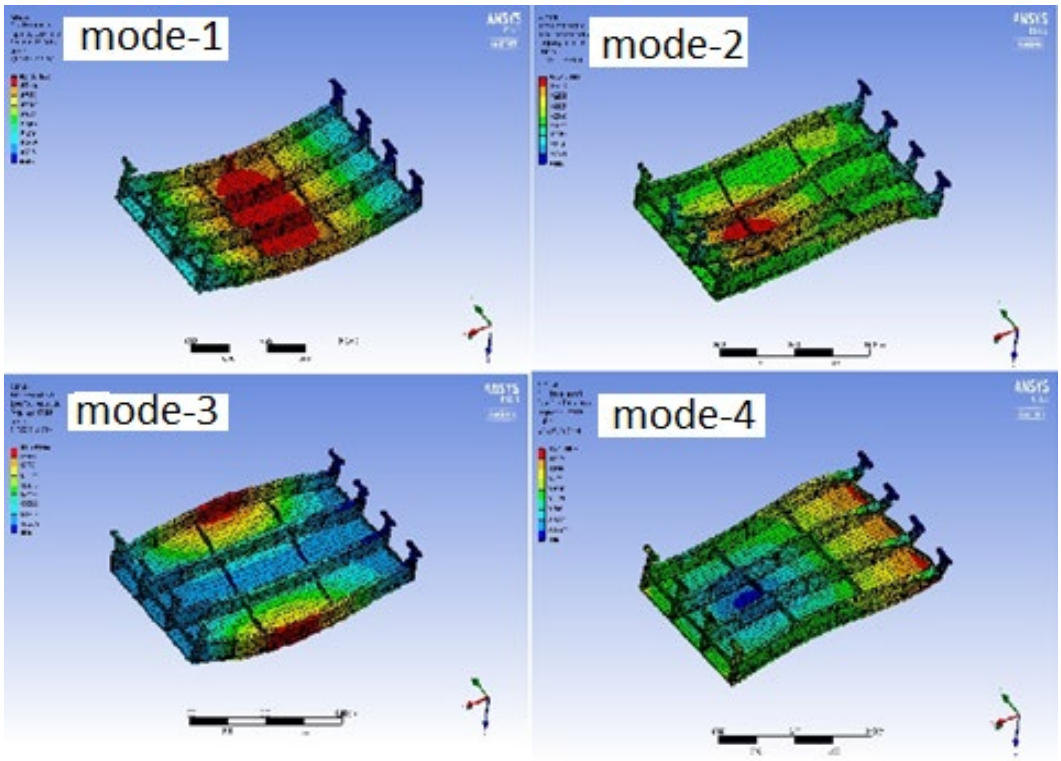

Figure 3.2 First few mode shapes of the model.

In order to test the efficacy of the proposed transmissibility-based damage-detection index, two damage scenarios were used with different severities. Each damage scenario is simulated by reducing the modulus of elasticity of the supports. In the first damage scenario (damage level 1), the modulus of elasticity was decreased by 10% for the inner two of the four supports at the left side of the model. In the second damage scenario, the modulus of elasticity of the four left supports was decreased by 10%. The DI calculation for both damage scenarios was based on Eq. 2.6, with all elements in the TR matrix, and Eq. 2.10. All elements in the TR matrix were calculated at frequencies where the coherence is high. It should be noted that the coherence functions of the out-of-diagonal elements in the TR matrix (Eq. 2.6) showed high values only at

narrow and limited frequency zones, while the diagonal elements in the TR matrix showed high coherence at a wider range of frequencies.

Figure 3.3 shows the resulting coherence functions (CF) of the different elements in the TR matrix (Eq. 2.6) and the transmissibility graphs of the different elements in the TR matrix for the intact (healthy) structure as well as for the structure with damage levels 1 and 2. In this 2x2 TR matrix, the first diagonal element represents the auto-acceleration component of TR, the second diagonal element represents the auto-angular velocity component of TR, and the out-of-diagonal element represents the cross acceleration-angular velocity component of TR.

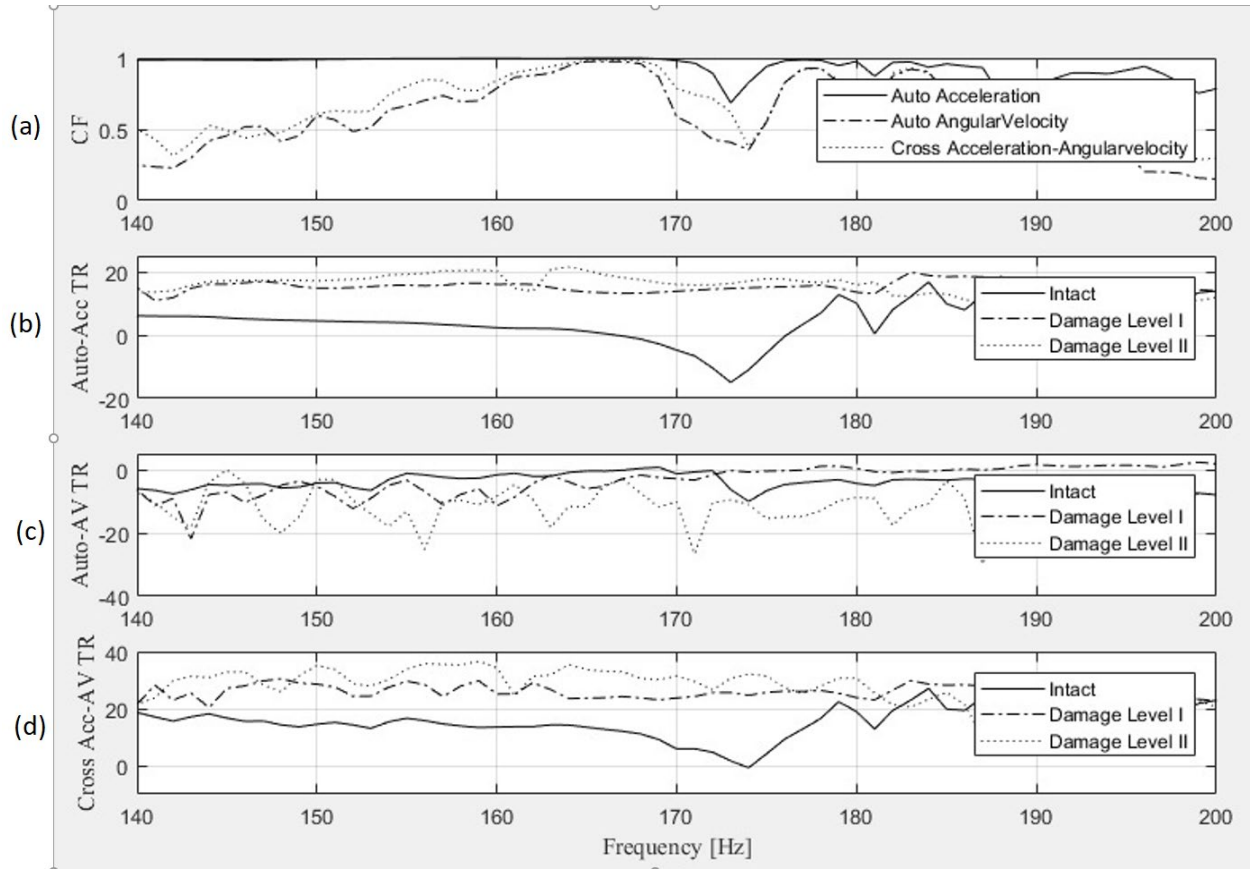

Figure 3.3 (a) The coherence function (CF) for the auto acceleration, auto angular velocity, and cross acceleration-angular velocity of the transmissibility (TR) matrix; (b) the first diagonal element of the TR matrix (the auto acceleration); (c) the second diagonal element of the TR matrix (the auto angular velocity) ;(d) the third diagonal element of the TR matrix (the cross acceleration-angular velocity).

Figure 3.4 shows the resulting damage index (Eq. 2.5) of each element in the TR matrix as well as the effective DI (overall TRs). As can be seen from the figure, the damage index of each element in the TR matrix was able to detect the damage. Some elements in the TR matrix, however, were not able to quantify the intensity of the damage, the auto-acceleration for example. Nevertheless, the effective DI (Eq. 2.10) was able to quantify the intensity of damage.

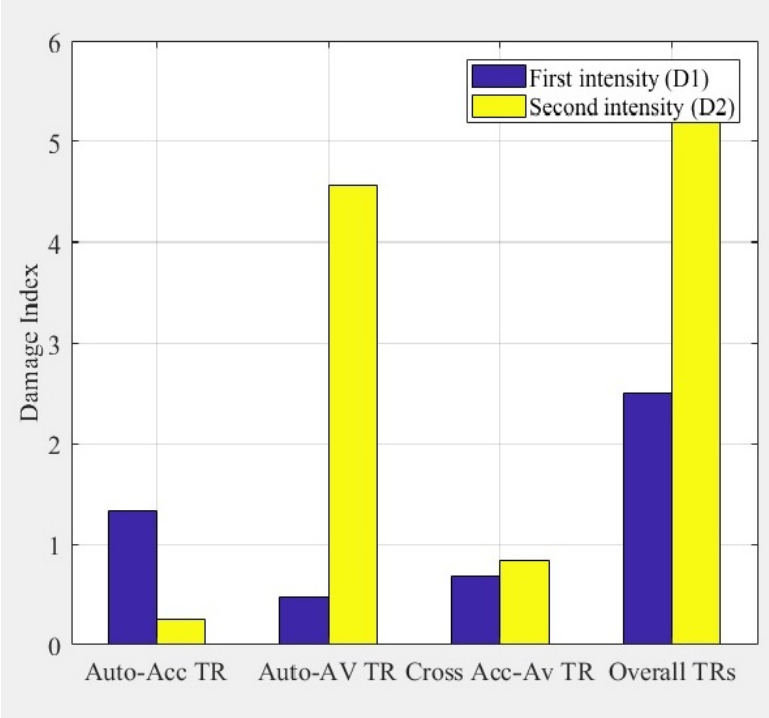

Figure 3.4 Damage index of the auto acceleration, auto angular velocity, cross acceleration-angular velocity, and the effective DI of the transmissibility (TR) matrix for the damage level 1 (D1) and damage level 2 (D2).

Chapter 4 Experimentation

In this work, the efficiency of the proposed damage-detection method was experimentally tested under different loading/damage conditions. Three types of sensors were installed on the model at different locations: accelerometers, gyroscopes, and strain gauges. The accelerometers and gyroscopes were attached on the girder of the bridge at two locations, as shown in figure 4.1, while the strain gauges were attached at the supports and the girder of the bridge (fig. 4.2).

First, the bridge model was tested under impact loading, where a wide range of frequencies can be introduced. Second, the model was tested on a shaking table that can simulate seismic scenarios. Finally, the model was tested in a water flume that can simulate flooding scenarios; in this case, the sensors (fig. 4.1c) and their associated data acquisition system (DAS) were sealed and protected from being submerged in the water/flume.

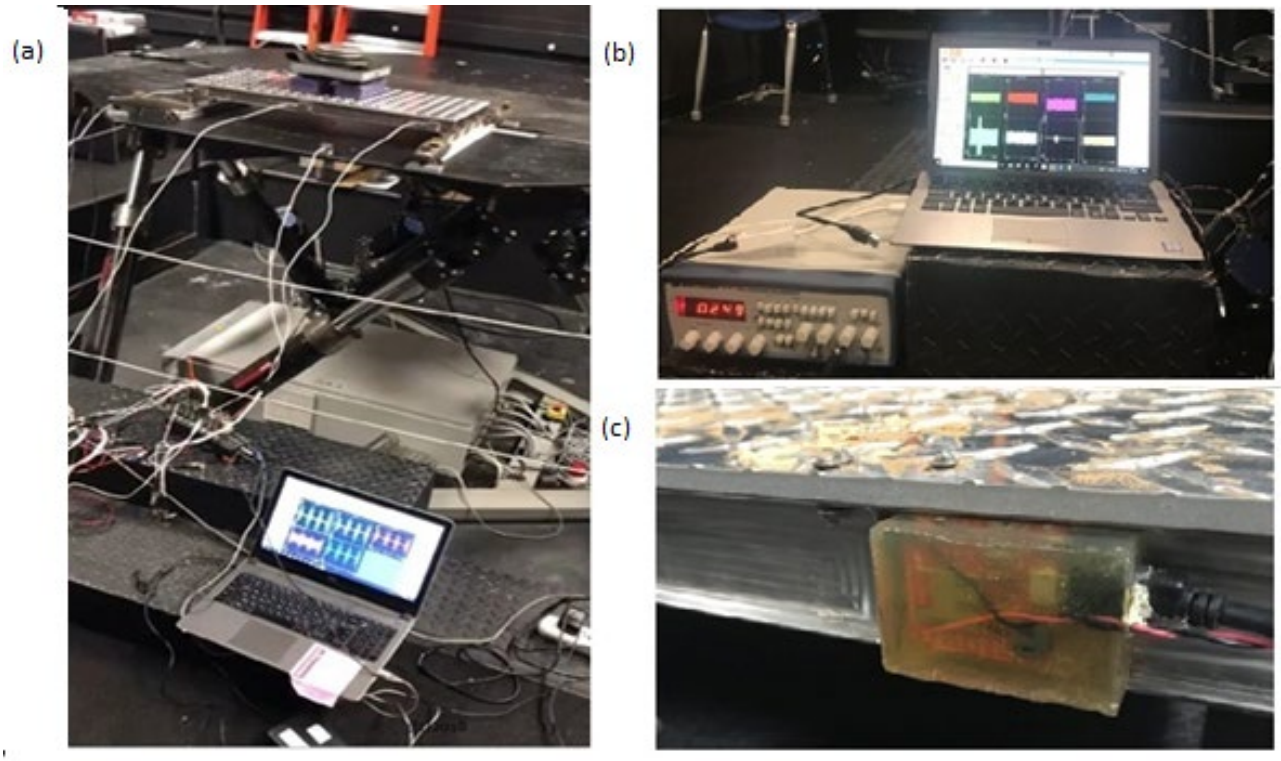

Figure 4.1 (a) The shaker setup testing, (b) the data acquisition system (DAS) and its associated trigger, (c) the waterproofed sealed accelerometer & gyroscope attached to the girder.

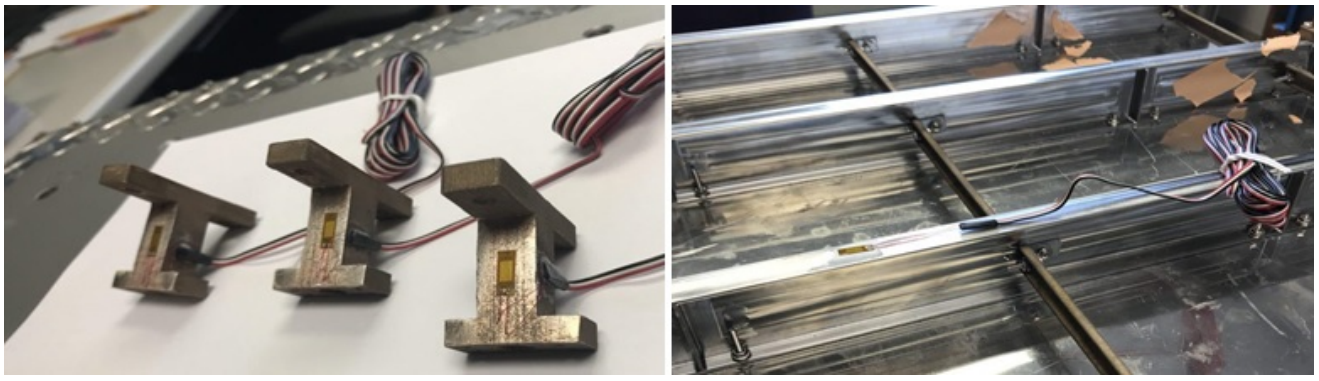

Figure 4.2 Strain gauges attached to the supports and girder of the bridge model.

4.1 Simulation of Damage

Two types of damage will be considered in the experimentation.

Damage Scenario I (System Mass Alternation): In the first damage scenario, the proposed damage-detection method is tested to sense the alteration in the mass of the system. In this scenario, the transmissibility of the intact (healthy) model (fig. 4.3a) was calculated. Then, one piece of mass (1 pound) was put on the deck of the model to simulate mass variation in the system and damage intensity level 1 (D1) (fig. 4.3b). Then, another piece of mass (1 pound) was loaded on the deck (fig. 4.3c) to simulate mass variation in the system and damage intensity level 2 (D2).

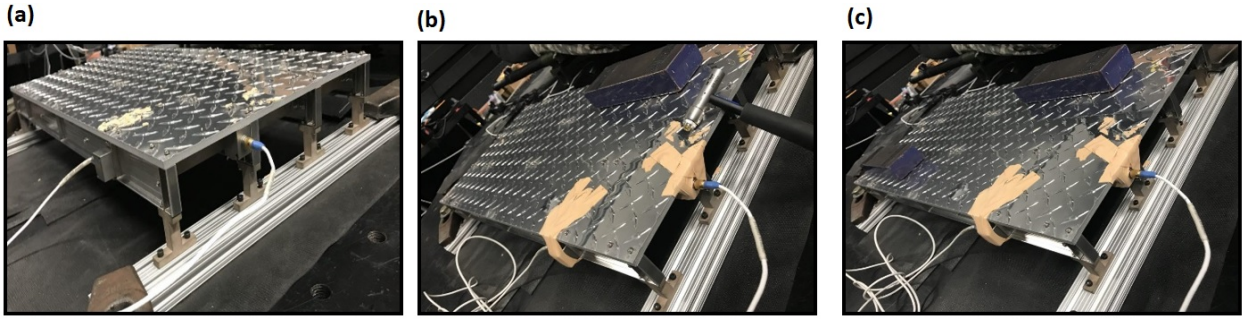

Figure 4.3 Simulating the mass alterations in the system (Damage Scenario I); (a) Intact model: without added mass; (b) Damage level 1 (D1): one piece of artificial mass was loaded; (c) Damage level 2 (D2): two pieces of artificial masses were loaded.

Damage Scenario II (System Stiffness Alteration): The second damage scenario was designed to check the efficiency of the proposed damage-detection method in sensing the variation in the stiffness of the system. In order to change the model stiffness realistically, it was decided to change the boundary conditions by loosening some bolts at the model bearing supports. In the initial step, the transmissibility of the intact model (fig. 4.4a) was calculated. The first level of damage (D1) was imitated by loosening and detaching bolts at a pair of bearing connections on the left side of the bridge model (fig. 4.4b). The second level of damage (D2) was

made by completely removing the bearing connection bolts on the left side of the model (fig. 4.4c).

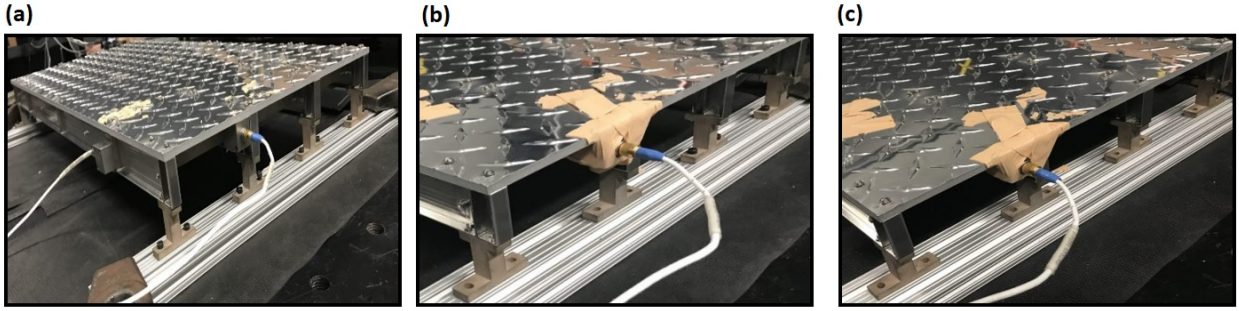

Figure 4.4 Simulating of the stiffness alteration in the system (Damage Scenario II); (a) Intact model: all bearing bolts were fastened; (b) Damage level 1: a pair of connections was loosened; (c) Damage level 2: all connections was loosened on one side of the model.

4.2 Experiment 1: Impact Test

In this test, the bridge model was rigidly attached to the platform of the shaker table. The bridge model was then subjected to an impulse force, using an impact hammer, at the center of the bridge. The damage was simulated using Damage Scenario I, where the damage intensity D1 and D2 were representing Damage Level 1 and Level 2, respectively. Figure 4.5 shows a sample result from an impact test for the transmissibility and coherence of the auto-acceleration and auto angular velocity. Figure 4.6 shows the damage index extracted from different sensors and the effective DI. In all experiments, the coherence function showed low magnitudes for the out-of-diagonal elements in the TR matrix. Therefore, the calculation of the effective DI will only be based on the diagonal elements of the TR matrix. As can be seen from figure 4.6, the magnitude of the DI for the strain sensors was much lower compared to other sensors.

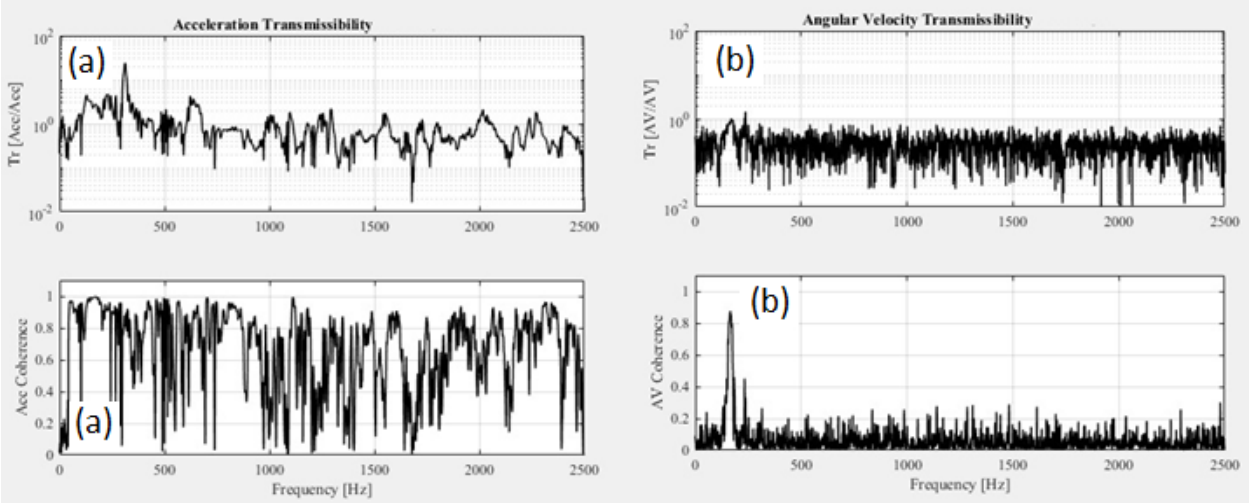

Figure 4.5 Transmissibility and coherence of the acceleration and angular velocity; (a) Acceleration TR and coherence function, (b) Angular velocity TR and coherence function.

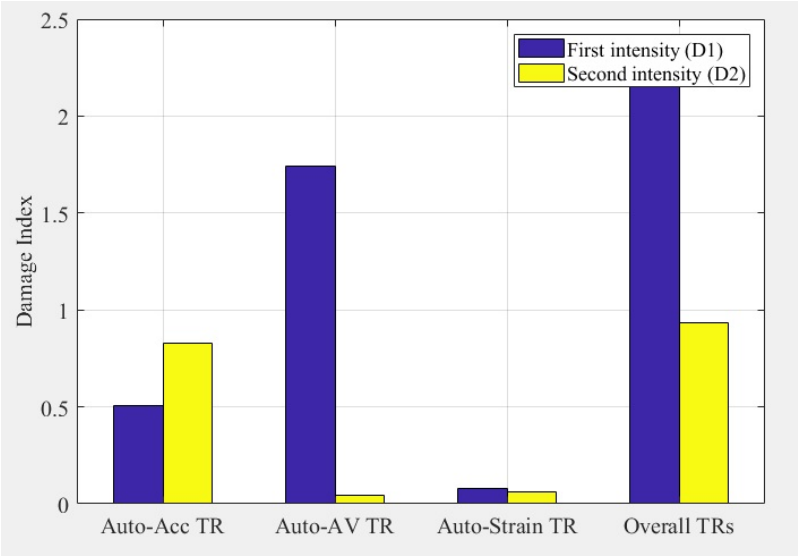

Figure 4.6 Damage index extracted from different sensors and the effective DI using Damage Scenario I with damage intensity D1 and D2.

4. 3 Experiment 2: Shaker Table Test

For the shaker test, the frequency band of excitation was limited; therefore, the results could be susceptible to the activities and noise at the low frequency range. Fig. 4.7 shows the

coherence functions (CF), the auto-acceleration TR, the auto angular velocity TR, and the auto strain TR. As can be seen from the figure, the high coherency bandwidth of each TR was different, but the method was able to diagnose those frequency ranges.

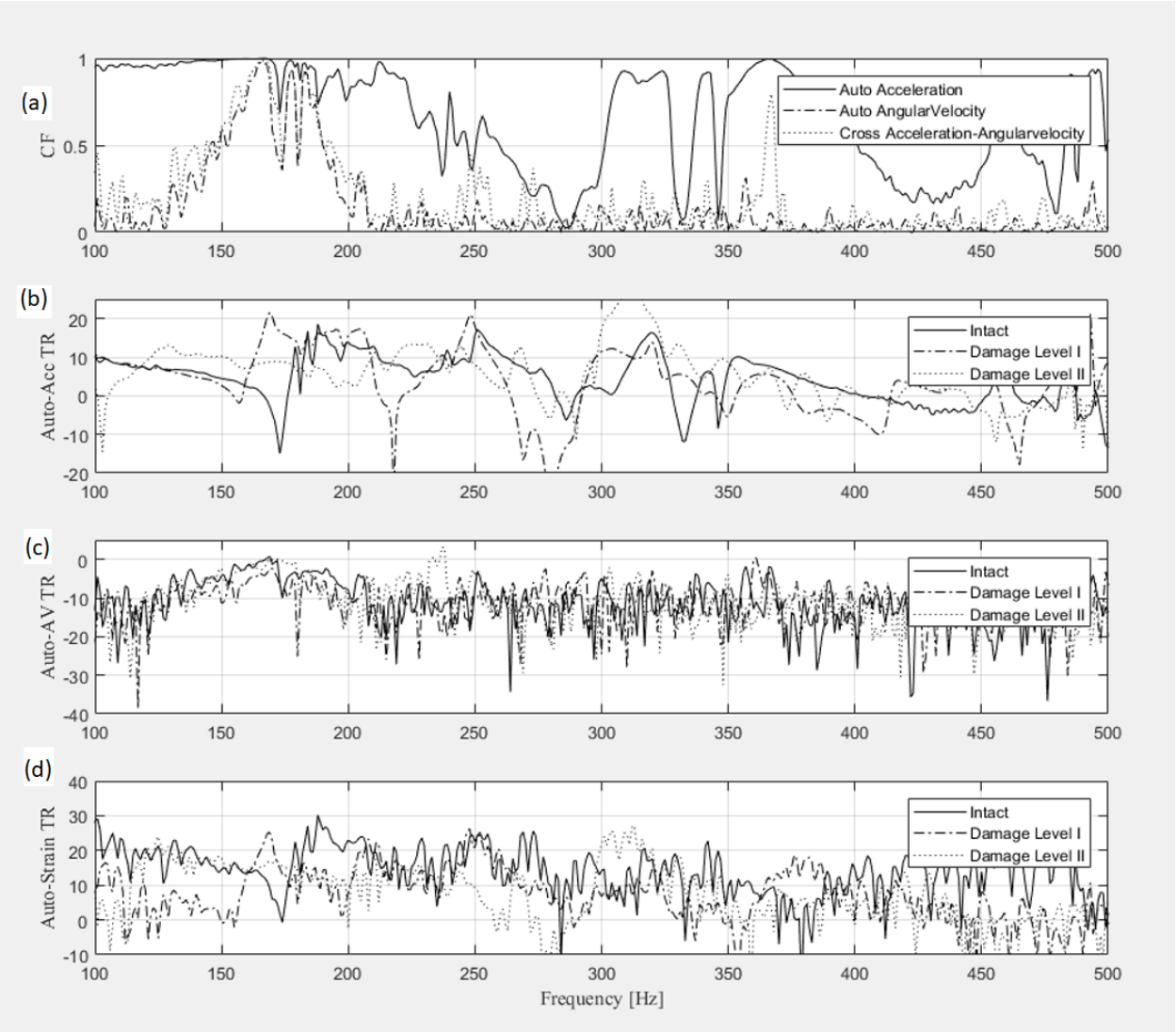

Figure 4.7 (a) coherence functions (CF), (b) auto-accelerations TR, (c) auto-angular velocity TR, and (d) auto-strain TR.

Figure 4.8 shows the damage index for the different components in the transmissibility matrix. Although the proposed method was able to detect damage, the intensity of the damage was diagnosed incorrectly for the auto-acceleration and auto-strain, which can be due to the limited frequency band of excitation. Still, the effective DI based on the overall diagonal components in the TR matrix was able to correctly quantify the damage intensity.

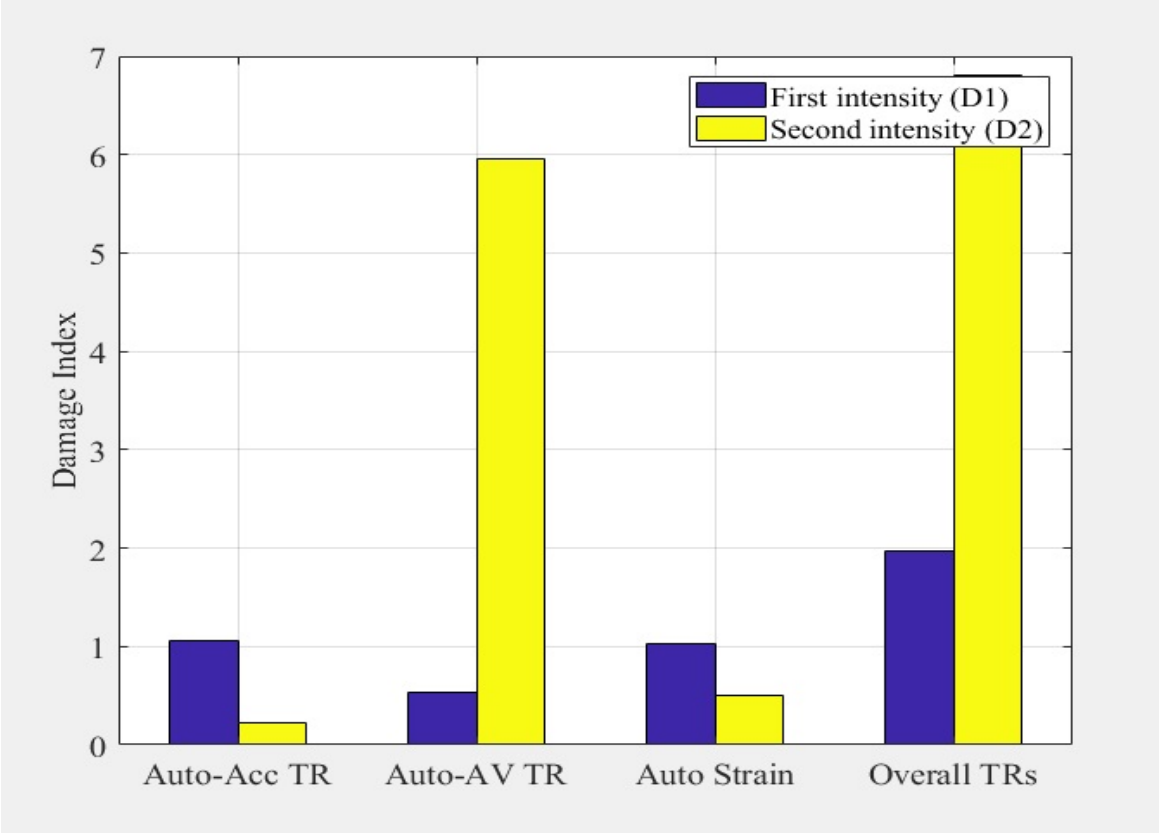

Figure 4.8 Damage index extracted from different sensors and the effective DI using Damage Scenario II with damage intensity D1 and D2.

4.4 Experiment 3: Water Flume Test

In this test, the bridge model was tested in a water flume to replicate conditions during possible extreme water events. The speed of the water inside the water flume can be controlled by changing the heights and angles of the flume (fig. 4.9).

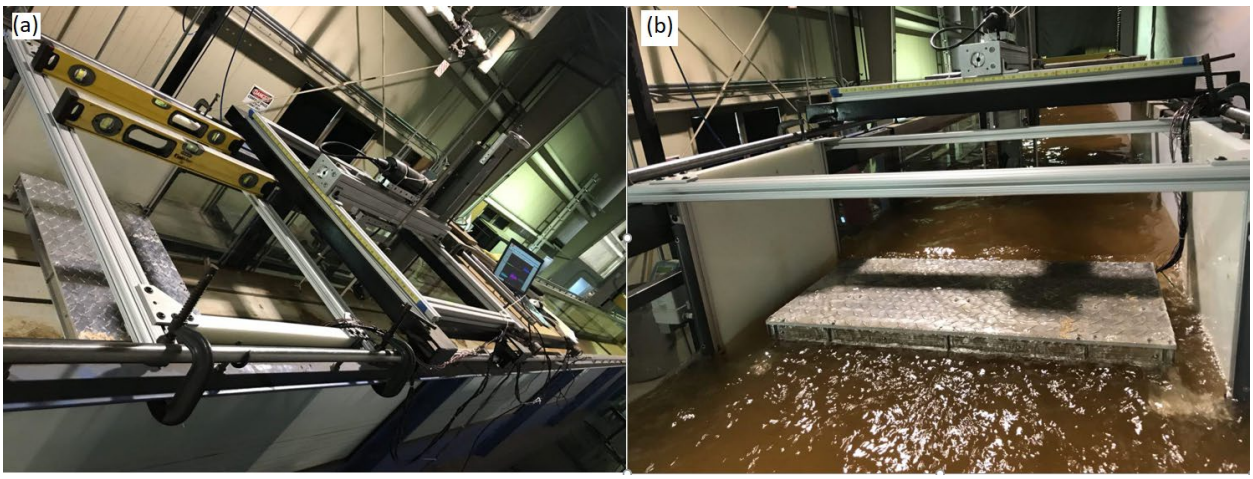

Figure 4.9 (a) The brace elements to mount the model in the flume, (b) the model during the low-velocity experiment.

One of the most critical issues for testing a structure in a water flume is instrumentation. Humidity and surrounding environments may affect the functionality and service life of the sensors. Therefore, all sensors were sealed and waterproofed and isolated by appropriate materials.

Figure 4.10 shows the transmissibility functions of the acceleration, angular velocity, and strain data for the healthy and damaged cases. Two damage scenarios (Damage Scenario I and Damage Scenario II) were considered. For each damage scenario, two levels of damage intensity (D1 and D2) were used.

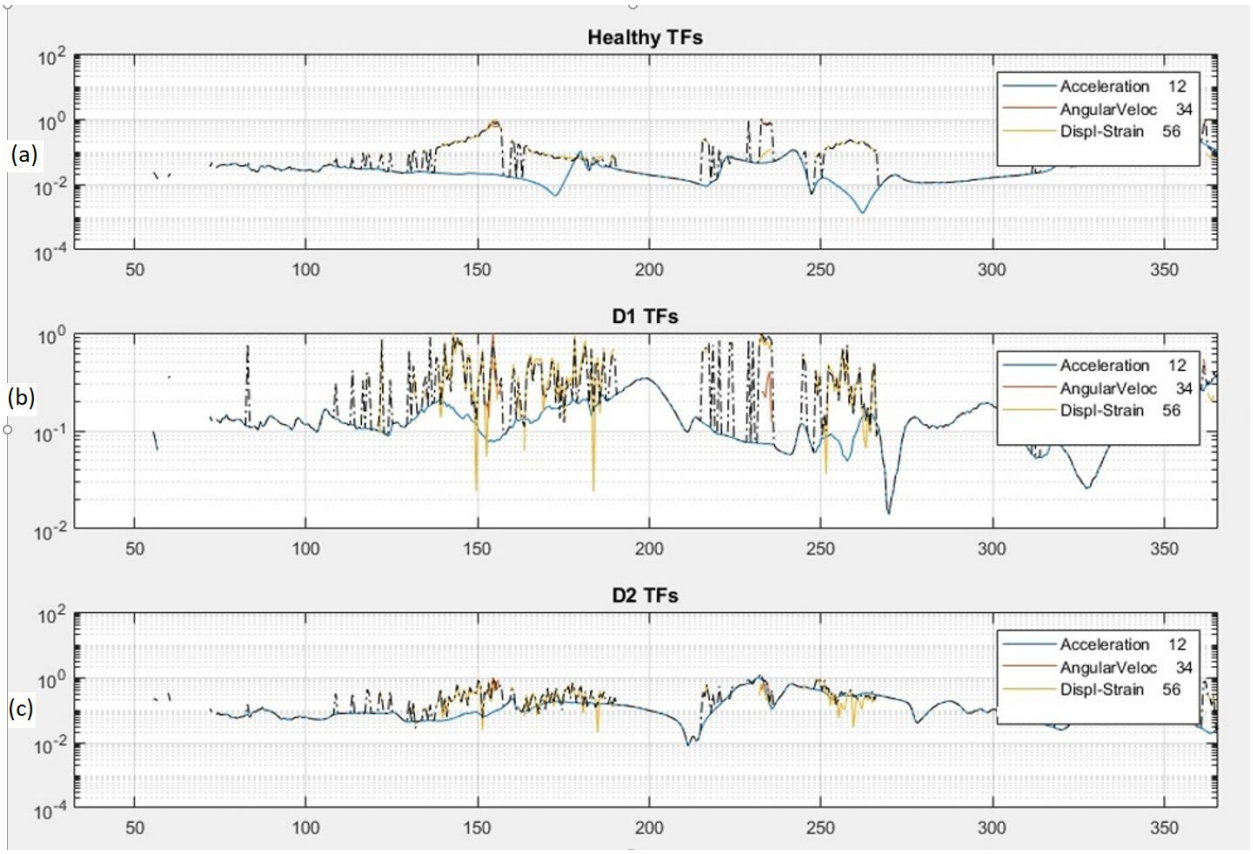

Figure 4.10 The transmissibility functions of the acceleration, angular velocity and strain data. Upper graph: Healthy, Middle graph: Damage Scenario II (D1), Lower graph: Damage Scenario II (D2).

The damage index for each TR was estimated alongside its high-coherency bandwidth. Figure 4.11 shows the damage indices produced from different transmissibility components due to different damage scenarios. Figure 4.11a shows the damage indices for Damage Scenario I with D1 and D2, while figure 4.11b shows the damage indices for Damage Scenario II with D1 and D2.

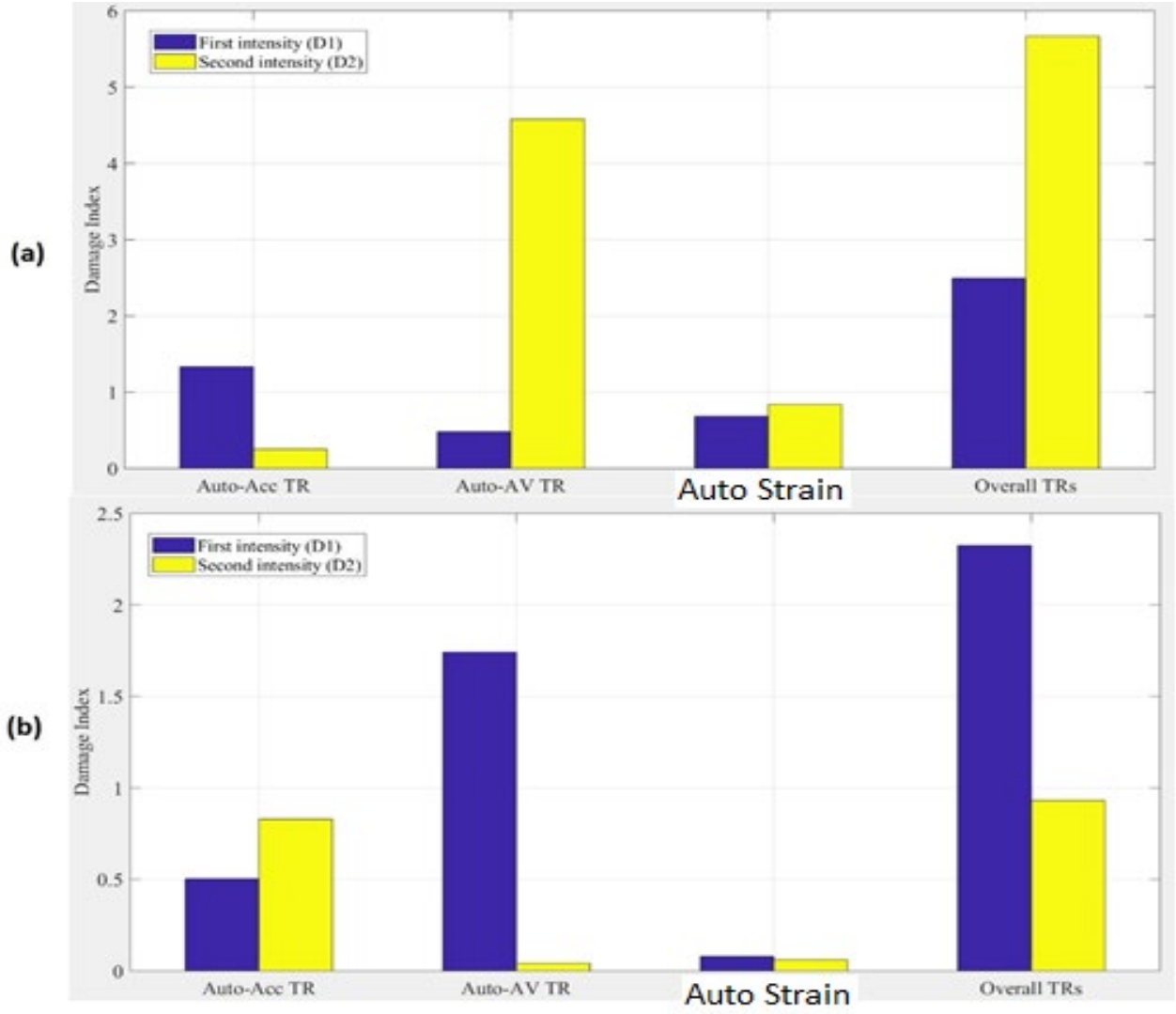

Figure 4.11 The damage indices estimated due to different predefined damage scenarios; (a) the system mass alteration (Damage Scenario I) with damage intensity D1 and D2; (b) the system stiffness alteration (Damage Scenario II) with damage intensity D1 and D2.

As can be seen from figure 4.11, the two damage scenarios had completely different outcomes. Each DI from each specific auto and cross TR acts differently in the two scenarios. In Damage Scenario I, only the auto angular velocity TR showed the severity of the damage. On the other hand, the auto acceleration TR and auto strain TR showed attenuated DI at the second level of damage (D2) incorrectly. However, because auto angular velocity DI was bold enough, the

total DI was able to manifest the damage intensity. In Damage Scenario II, only auto acceleration TR was able to show the damage intensity correctly. Other DIs from other TRs either decreased or stayed constant at the second level of damage (D2). The overall DI also has been dropped for the second level of damage (D2) incorrectly.

Chapter 5 Discussion and Conclusion

This work investigated the transmissibility-based damage-detection method and the proposed effective damage index (Effective DI) when multiple sensors were used. In this work, acceleration, angular velocity, and strain signals were recorded. The proposed effective DI consolidates the damage indices from all sensors into one effective index. The validity of the proposed effective DI was tested on a small scale model of a highway bridge under impulse loading, with ground motion, and inside a water flume.

The results were different in some simulated damage scenarios. The results of the test in the water flume showed that DI from auto angular velocity TR was more sensitive to mass changes in the system than auto acceleration. It was also more sensitive to stiffness changes in the system than auto angular velocity. It should be noted that these results could be affected by the low energy of the excitation forces inside the water flume and may not represent a standard trend. Generally speaking, the results showed that using multiple sensors may generate a better chance to capture the changes in the integrity of the structure rather than using one type of sensor. Some sensors perform differently depending on their location on the structure, the severity of motion and deformation, and their sensitivity to noises and environmental effects. For example, the signal-to-noise ratio in the strain gauges is expected to be very small, especially when the structure is subjected to a low level of loading, just like the situation with the testing in the water flume. The acceleration and angular velocity signal quality may also suffer under the shaker table test and the water flume test as the excitation forces may generate activities at lower frequencies that may not excite the higher modes of the structure. The proposed Effective DI will be tested and refined in future work.

References

1. Farrar, C. R., and Lieven, N. A. J., Damage prognosis: The future of structural health monitoring. Phil. Trans. R. Soc. A, 2007, 365(1851): 623–632.

2. Fan, W., and Qiao, P. Z., Vibration-based damage identification methods: A review and comparative study. Struct. Health Monit., 2011, 10(1): 83–111.

3. Xu YL, et al. Testbed for structural health monitoring of long-span suspension bridges, Journal of bridge engineering, 2012, 17(6): 896-906.

4. Hong, W. et al., Finite element model updating of flexural structures based on modal parameters extracted from dynamic distributed macro-strain responses, Journal of Intelligent Material Systems and Structures, 2015, 26(2): 201–218.

5. Hong, W., Wu, Z., Yang, C., and Wu, G., Finite element model updating of flexural structures based on modal parameters extracted from dynamic distributed macro-strain responses, Journal of Intelligent Material Systems and Structures, 2015, 26(2): 201-218.

6. Brincker, R., and Ventura, C., Introduction to operational modal analysis, John Wiley & Sons, 2015.

7. Avitabile, P., Modal Testing (A practitioner's guide), John Wiley 2018.

8. Brandt, A., Noise and Vibration Analysis (Signal Analysis and Experimental Procedures), 2011, John Wiley & Sons, Ltd.

9. Wang, T., Celik, O., and Catbas, F.N., Damage detection of a bridge model based on operational dynamic strain measurements, Advances in Structural Engineering, 2016, 19(9): 1379-1389.

10. Lee, E., Rahmatalla, S., and Eun, H., Damage detection by mixed measurements using accelerometers and strain gages, Smart Struct, 2013, 22: 075014.

11. Maia, N.M.M., Urgueira, A.P.V., and Almeida, R.A.B., Whys and Wherefores of Transmissibility, Vibration Analysis and Control – New Trends and Developments, InTech, 2011, 197–216.

12. Johnson, T.J., and Adams, D.E., Transmissibility as a differential indicator of structural damage. J Vib Acoust, 2002, 124(4): 634–641.

13. Maia, N.M.M., Almeida,. R., Urgueira, A., and Sampaio, R., Damage detection and quantification using transmissibility, Mechanical Systems and Signal Processing, 2011, 25: 2475–2483.

14. Zhou, Y.-L., Figueiredo, E., Maia, N.M.M., Sampaio, R., and Perera, R., Damage detection in structures using a transmissibility-based Mahalanobis distance, Struct Control Health Monit, 2015, 22: 1209–22.

15. Zhou, Y.-L., Figueiredo, E., Maia, N.M.M., and Perera, R., Damage detection and quantification using transmissibility coherence analysis, Shock and Vibration (Article ID 290714), 2015.

16. Zhou, Y.-L., Maia, N.M.M., and Wahab, M.A., Damage detection using transmissibility compressed by principal component analysis enhanced with distance measure. J Vib Control, 2016, http://dx.doi.org/10.1177/1077546316674544.

17. Cheng, L., Busca, G., Roberto, P., Vanali, M., and Cigada, A., Damage Detection Based on Strain Transmissibility for Beam Structure by Using Distributed Fiber Optics, 2017, IMAC Structural Health Monitoring & Damage Detection, Volume 7, DOI 10.1007/978-3-319-54109-9_4.

18. Schallhorn, C., and Rahmatalla, S., Damage detection of retrofitted crack re-initiation and growth, S. J Civil Struct Health Monit (2015) 5: 377.

19. Schallhorn, C., and Rahmatalla, S., Crack detection and health monitoring of highway steel-girder bridges, Structural Health Monitoring, 2015, 14(3): 281 – 299.

20. Zhou, Y.-L., Wahab, M.A., Cosine based and extended transmissibility damage indicators for structural damage detection, Engineering Structures, 2017, 141: 175–183.

21. Zhou, Y.-L., Maia, N.M.M., Sampaio, R.P.C., and Wahab, M.A., Structural damage detection using transmissibility together with hierarchical clustering analysis and similarity measure, Structural Health Monitoring, 2017, 16(6): 711–731.

22. Glaser, S. D., Li, H., Wang, M. L., Ou, J. P., and Lynch, J. Sensor technology innovation for the advancement of structural health monitoring: a strategic program of US-China research for the next decade, Smart Struct. Sys., 2007, 3(2): 221-244.

23. Rahmatalla, S., Hudson, K., Liu. Y., and Eun H.-C., Finite element modal analysis and vibration-waveforms in health inspection of old bridges, Finite Elements in Analysis and Design, 2014, 78: 40–46.